Advances in Research
7(6): 1-17, 2016, Article no.AIR.27351
ISSN: 2348-0394, NLM ID: 101666096

SCIENCEDOMAIN *international*
www.sciencedomain.org

A Review: Optical Second – Harmonic Generation Enhancement via Plasmonic Surface - Theory and Applications

Nadia Mohammed Jassim[1*]

[1]*Department of Physics, College of Science, University of Diyala, Iraq.*

Author's contribution

The sole author designed, analyzed and interpreted and prepared the manuscript.

Article Information

DOI: 10.9734/AIR/2016/27351
Editor(s):
(1) Martin Kroger, Professor Computational Polymer Physics, Swiss Federal Institute of Technology (ETH Zurich), Switzerland.
Reviewers:
(1) Yanjun Liu, Institute of Materials Research and Engineering, Singapore.
(2) Di Feng, Beihang University, Beijing, China.
(3) Wenhua Gu, Nanjing University of Science and Technology, China.
(4) N.E.J. Omaghali, University of Jos, Nigeria.
Complete Peer review History: http://www.sciencedomain.org/review-history/15966

Review Article

Received 30th May 2016
Accepted 16th August 2016
Published 27th August 2016

ABSTRACT

Plasmonics has arisen as an interested research field in nanoscience and nanotechnology with many potential applications in fields ranging from bioscience, information processing and communication to quantum optics. It is based on the generation, manipulation and transfer of surface plasmons (SPs) that have the ability to manipulate light at the nanoscale. Realizing plasmonic applications requires comprehension how the SP-based properties depend on the nanostructures and how these properties can be controlled. Lately, significant attention has been devoted to the noteworthy and the comprehensions of nonlinear optical processes in plasmonic nanostructures, giving create to the new research field called nonlinear plasmonics. This review article gives a comprehensive understanding of physical mechanisms of one of these nonlinear optical processes, namely, second harmonic generation (SHG), with an focusing on the main differences with the linear response of plasmonic nanostructures. The main applications, ranging from the nonlinear optical characterization of nanostructure shapes to the optimization of laser beams at the nanoscale, are summarized and discussed. Future directions and developments,

**Corresponding author: E-mail: Jassim@Sciences.uodiyala.edu.iq;*

made possible by the unique combination of SHG surface sensitivity and field enhancements associated with surface plasmon resonances, are also addressed.

Keywords: SHG; nonlinear plasmonics; plasmonic resonance PR; Localized surface plasmon LSP; SHG enhancement; damage threshold.

1. INTRODUCTION

The plasmonic field interest of the study of the optical properties of metallic nanoparticles. Collective oscillations of the quasi-free conduction electrons with respect to the fixed ionic background can be excited by an external light field. This displacement of charges leads to strong local electric fields in nanoscale volumes around the nanoparticles. Due to the large resonant dipole moment, which is fundamentally connected to the large number of free conduction electrons, energy can be efficiently channeled from the far-field into the so-called near-field. There are previously discussed indicate the strong local fields produces a many phenomena and applications : The plasmonic resonances in arrangements of multiple nanoparticles can couple together giving rise to collective modes similar to molecular physics, which led to the development of the so-called plasmon hybridization model [1]. One can also transport energy on deep subwavelength length scales, create the plasmonic analogue of electromagnetically induced transparency (EIT), and construct systems with tailorable near-field enhancement and confinement. What is more, the resonant behavior of plasmonic particles is partially determined by the refractive index of the surrounding environment, enabling plasmonic refractive index sensing utilizing ensembles of nanoparticles as well as individual nanostructures. As found, the improved of the local electric field strength lead to efficient of the nonlinear optics in these systems as the radiated intensities scale nonlinearly with the fundamental driving light field [2].

A nonlinear optical process, namely, the generation of second harmonic light (SHG) from a metal (silver) surface was first observed in 1965 [3], four years after the first observation of SHG from quartz in 1961 [4]. In the following fifty years, a many of interest properties of SHG from metallic surfaces have been founded such as (1) second harmonic (SH) intensities can be improved more than an order of value by coupling incident light into surface polariton resonances at metal surfaces [5]; (2) SHG from surfaces of centrosymmetric metals is anisotropic, the strength of the SH response thus depends on the relative orientation of the incident field and the crystal axes [6,7]; (3) Because of local-field enhancement, SHG is very sensitive to surface roughness and chemical processes such as adsorption and electrochemical reactions [8,9]. On the theoretical side, different approaches on both phenomenological and microscopic levels have been developed to analyze SH response from metals [10], such as classical Boltzman equation approach, hydrodynamic model [11,12,13], phenomenological formalism in terms of the fundamental tensor elements of the SH susceptibility [14,15,16] and the self-consistent density functional formalism [17].

The nonlinear optical properties play an important role in photonics, materials science, and bioimaging with potential applications such as frequency mixing, super continuum generation, and optical solitons. Second-harmonic generation (SHG) is the lowest order frequency mixing nonlinear optical process where two photons create a single photon with half the incident wavelength [18-22]. This gives a *suitable*, *proper* and practical sense to get blue emission from a near-infrared laser and has found applications as nonlinear optical frequency converters, all-optical signal processors, and biosensors. Specifically, achieving SHGs with nanowires/nanobelts (e.g., in ZnO, GaN, GaP, and $KNbO_3$) would prove highly advantageous for nanoscale coherent light sources and integrated optical circuits [23-26]. Moreover, light-emitting nanoscale probes have also been selected as an ideal platform for single-molecule fluorescence imaging, single-molecule endoscopy, and in vivo cell imaging [27-30]. However, SHG is generally inefficient at such diminutive scales. Many schemes to enhance SHG in nanostructures (e.g., utilizing the Purcell effect, structure tailoring, interface strain and plasmonic effects) have already been proposed to exceeded this serious restriction. Among them, utilizing plasmonic effects is especially compatible with the localization of highly concentrated local fields at resonance in the compact mode volumes of these nanostructures. Plasmonics, which includes the coupling

between electromagnetic radiation and collective electronic oscillations (or surface plasmons) in metals, is also related for the manipulation of light at the nanoscale. Plasmonic structures enhance the nonlinear effects in the following ways: (a) such nanostructures provide field enhancement near the metal-dielectric interface, coupled with the excitation of either surface plasmon polaritons (SPPs) or localized surface plasmons (LSPs), or (b) the nonlinear change of the refractive index in either material can greatly modify plasmonic resonances and coupled reflection, transmission, or absorption of light. Currently, most works on enhancing nonlinear effects are either concentrated on the metal nanostructures (e.g., nanoaperture silver film, gold bowtie antenna, non-centrosymmetric gold nanocup, gold gratings, and tapered plasmonic silver waveguide) or concentrated on enhancing the nonlinear properties of semiconductors at the single nanoscale structure level (e.g., SHG from single core-shell quantum dots, ZnO nanowire, $KNbO_3$ nanowire, and $KTiOPO_4$). Studies on enhancing the SHG from a single nanostructure using plasmonic effects are rarely reported. To the best of our knowledge, these studies contain (a) the demonstration of large enhancement of SHG in $BaTiO_3$/Au core-shell structures benefit the entire mode volume for an even-order nonlinear optical process, (b) the detection of a second order optical response from a single sphere comprising a centrosymmetric material coated with a nonlinear material, (c) the generation of high efficiency second-harmonic responses from a single hybrid ZnO nanowire/Au plasmonic nano-oligomer, (d) enhanced nonlinear response of single GaAs nanowires by coupling to optical nanoantennas, and (e) enhanced optical signal in the near-infrared spectral range by using a $KNbO_3$-Au core-shell structure. Laterally, enhanced second-harmonic generation from metal-integrated CdS semiconductor nanowires was studied by the highly confined whispering gallery modes [22].

2. NONLINEAR PLASMONICS

In the optical nonlinear effects, the electronic motion forces in electromagnetic waves are non harmonic. Expansion of the anharmonicity as power series in the electromagnetic waves [31] mixes the incident waves and produces new waves that oscillate at the sums and differences of the essential frequencies and can oscillate with different directions (Fig. 1).

In the nonlinear regime, the expression for the material polarization *P* should be modified to a power series as,

$$P = \varepsilon_0 \left[\chi^{(1)} E + \chi^{(2)} E^2 + \chi^{(3)} E^3 + \cdots \right] \quad (1)$$

Where, E is the optical field, $\chi^{(n)}$ is the nth-order susceptibility of the material and ε_0 is the vacuum permittivity. The optical process includes the harmonic time with the different frequencies, ω_n. The first term in equation (1) represent to the linear response process, where each component excites to polarization oscillating at the specific frequency. This term describes the optical linear process. For instance absorption, scattering and refraction processes. The others terms in equation (1) represent to the higher-order, where (n>1). The high order includes sums and differences of the incident frequencies and the excitation of

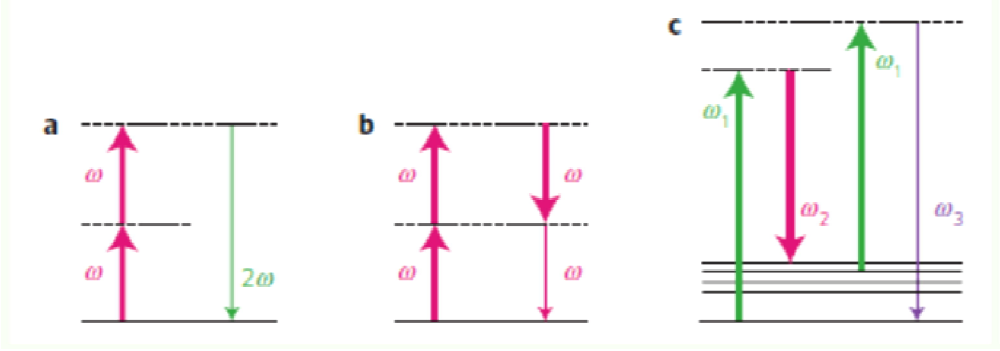

Fig. 1. The nonlinear processes of photon diagrams adapted from reference [32]: a, represent to SHG diagram, b, FWM degeneration diagram, c, the vibrational energy molecules of Raman Scattering

radiation at new frequencies. The positive and negative frequencies combine is described by the photon diagrams (Fig. 1). The second-order susceptibility $\chi^{(2)}$ includes the sum and difference frequency generation, second harmonic generation, and optical parametric amplification. The above-mentioned second-order nonlinear effects are created by two waves, which interact to create a third wave. Conservation of momentum and photon energy are always required in these processes. The optical fields of these waves are coupled to one another through the second-order susceptibility. The coupling provides the mechanism for the exchange of energy among the interacting fields. In centro-symmetric crystals, $\chi^{(2)}$ is zero; therefore second-order nonlinear processes are generally possible only in materials that lack inversion symmetry.

Table 1. Second –order nonlinear optical susceptibility $\chi^{(2)}$ for several crystals

Material	Point group	d_{il}(pm/V)
Ag_3AsS_3 (proustite)	3m = C_3v	d_{22} = 18 d_{15} = 11
$AgGaSe_2$	$\bar{4}2m$ =D_{2d}	d_{36}=33
$AgSbS_3$ (pyrargyrite)	3m = C_{3v}	d_{15} = 8 d_{22} = 9
beta-BaB_2O_4(BBO) (beta barium borate)	3m = C_{3v}	d_{22} = 2.2
$CdGeAs_2$	$\bar{4}2m$ =D_{2d}	d_{36} = 235
CdS	6mm =C_{6v}	d_{33} = 78 d_{31} = - 40
GaAs	$\bar{4}3m$	d_{36} = 370
KH_2PO_4 (KDP)	2m	d_{36} = 0.43
KD_2PO_4 (KD*P)	2m	d_{36} = 0.42
$LilO_3$	6 = C_6	d_{15} = - 5.5 d_{31} = -7
$LiNbO_3$	3m = C_{3v}	d_{32} = - 30 d_{31} = - 5.9
Quartz	32 = D_3	d_{11} = 0.3 d_{14} = 0.008

When single nonlinear sources add to phase, the nonlinear response get to strong and coherent signals. Phase matching is representing to the frequency conversion and materials much larger than the wavelength. By other means, the nonlinear effects are only over the coherence length of the interaction, such as on the order of 10 μm. For subwavelength nonlinear sources the signals of the nonlinear sources are emitted in all direction, so the phase-matching s is not interesting. As well as the random ensembles of subwavelength sources signals are also emitted in all directions (hyper-scattering). Indeed, the optical field seen by a consider dipole in the material is not the same as the macroscopic field. The local field at frequency ω_n and point r is following:

$$E_{loc,\,i}(\omega,\mathbf{r}_n) = \sum_j L_{ij}(\omega,\mathbf{r}_n)\, E_j(\omega_n) \tag{2}$$

Where i and j refer to cartesian components of the field. The frequencies are merits of the field. The local field factor, $L_{ij}(\omega_n, r)$, is tensorial, as the field direction may also change through local-field effects which important in nanostructures materials and can enhancement the local-field distribution, for example when a surface plasmon is excited.

For potential applications, there are many interest effects occur at second and third order. The second-order response excites the wave-mixing effects that a result of the conversion frequency, the important example is the second harmonic generation (SHG) also called frequency doubling, where the incident photon frequency, ω, is converted to its second harmonic, 2ω. Also there are frequencies arise from third-order nonlinearities effects. The third-order response contains terms is called the optical Kerr effect at the incident frequencies. Due to the modification of the refractive index, the all- optical switching and light modulation are allowing by making together the optical cavities and kerr nonlinearities. This is lead to get bistability, where one input signal allows two potential outputs. The plasmonic structures can improve nonlinear effects by two methods. (1), such structures give field enhancement near the metal–dielectric interface, coupled with the excitation of surface plasmon, which based on the frequency-dependent local-field factor $L(\omega, r) = |E_{loc}(\omega, r)/E_0(\omega)|$, where r is represent to the position vector, $E_{loc}(\omega, r)$ is represent to the local field at frequency ω coupled with the plasmonic excitation, and the incident field is referred to $E_0(\omega)$. The nonlinear optical locally response is causing the strong enhancement when the optical response is whole integrated in the material, this lead to the increasing of the metal the metal nonlinearity (intrinsic response) or of a material adjacent to the metal (extrinsic response). (2), the surface plasmon and metamaterial resonance frequency, are depending on the refractive indices of the metal

and the surrounding dielectric. These nonlinear changes in the index material lead to modify plasmonic resonances and coupled reflection, transmission or absorption of light. The nonlinear effects are depending on the symmetry of materials [31]. The second and third order effects are possible only in non-centrosymmetric materials within the electric-dipole approximation of the light–matter interaction. The magnetic and quadrupole effects allow second-order effects even in centrosymmetric materials, these effects are difficult to get. The plasmonic effects can achieve the nonlinear optical response by creating the oscillations of conduction electrons at the metal surface structures [33,34]. The optical properties of nanostructures are depending on the incident electromagnetic field and the coherent motion of free-electron plasma at the metal surface. A surface plasmon polariton (SPP) is a propagating surface wave at the interface of the metal–dielectric (Fig. 2).

The electromagnetic field decays exponentially on both sides of the interface, this leading to the confinement subwavelength at the metal surface. On two-dimensional planar interfaces, the surface plasmon polaritons is a longitudinal wave with electric field components both verticaly to the metal interface and parallel to the wavevector. There are many requirements to get an electric field component in the plane of incidence for SPP excitation. The SPP wavevector is larger than the wavevector of light propagating in the surroundingt dielectric medium. Coupling of light from free space to SPPs, in analogy with every kind of guided photonic modes, therefore requires special arrangements such as a prism or diffraction grating coupler. Given to its dispersion, an SPP is a slow wave accumulating energy from the incoming light and providing field enhancement near the metal interface. Consequently of ohmic losses in metal, SPPs have a finite propagation distance that based on the geometry of the supporting structure. The enhancement, can be achieved by choosing the suitable interface between the metal and the dielectric medium. By carry out so, it is probable to make plasmonic waveguides and plasmonic crystals [33] (periodically structured plasmonic surfaces or films).

Localized surface plasmons (LSPs) are non propagating excitations of the conduction electrons of metal nanoparticles, which depend on the size, shape and refractive index of their surroundings. Due to the confined at the surface nanoparticle, LSPs has a small mode volume and lead to the enhancement of the electromagnetic wave, which is limited by ohmic and radiative losses [33] as well as quantum [34] and nonlocal [35] effects in the case of ultra small sizes. LSPs are important subwavelength advantages on a metal surface. LSP have an important case in the behaviour of SPPs on rough surfaces at the resonances frequencies. The interaction between the resonances frequencies referred to the spectrum of LSPs coupled with an ensemble of metallic particles. The enhancement of the electromagnetic waves depend on the shape and size of the single particles and the distance between them [36-38].

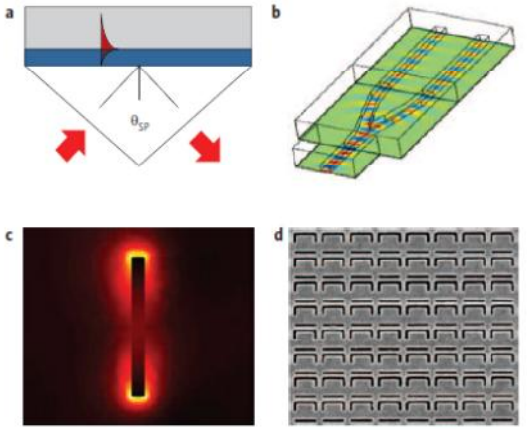

Fig. 2. Plasmonic structures diagrams. a, Surface plasmon polaritons (SPP) diagram of a planar metal film by a prism b, Electric field distribution of the SPP mode in a dielectric-loaded plasmonic waveguide-splitter. c, Dipolar localized surface plasmon LSP mode intensity distribution of nanorod-shaped particle. Brighter color depends on the intensity. d, Scanning Electron Microscopy SEM image of a plasmonic metamaterial [32]

3. SECOND-HARMONIC GENERATION (SHG) IN NANOSTRUCTURES

The first termed of electromagnetic second harmonic scattering (hyper-Rayleigh scattering (HRS)) from small spherical particles was studied the localized surface plasmon that depended on Mie theory [39]. This formalism of the local bulk response [40] put selection rules for signals creating from the various multipolar Mie terms at the second-harmonic wavelengths. There are some applications of HRS [41] 13 nm gold NPs led to hyperpolarizability of 2,000–3000 × 10^{-30} e.s.u. per atom, considering that the best

molecular materials. 32 nm Ag NPs was used to study the Interference between dipolar and quadrupolar HRS [42]. A lot of studies were used particles ranging 20 to 150 nm have demonstrated that small, non-spherical particles have a dipolar response creating from haven't centrosymmetry [43]. For large particles, field retardation across the particle enhances the quadrupole interaction, allowing HRS even from spherical particles. Lately, this interaction between multipoles has also been expanded to octupoles [44]. Since these kit experiments, HRS from single gold NPs has been noticed [45]. Because of HRS different resonance properties The different multipoles are critical. For instance the quadrupole resonances have narrower line widths than the normal dipole resonances but are weaker. Regrettably, the quadrupole resonance usually takes place at the spectral onset of the dipole resonance and hence hardly resolved. The selection rules of HRS can be used to isolate the quadrupolar signal. This provides the opportunity a potential for nonlinear sensing of the refractive index of the ambient with features superior to those of classical methods [46].

There are many studies on non-spherical plasmonic have been achieved. SHG from the sharp tip of a gold nanocone was highest light polarized along the tip axis [47], as expected, as a result of the lowered symmetry relative to the sphere [48]. The advanced structure of SHG consisted of a nano-aperture in Ag film surrounded by a concentric grating [49] (Fig. 3a). The grating guided the incident light to the aperture; in this case the SHG response was enhanced by four orders of magnitude compared without uses of grating. The role of the nanogap between two nanospheres was investigated by FWM [50]. The gap size decreased as signal increased to the angstrom regime, where quantum effects start limiting the local-field enhancement [51]. The geometry of nanoantennas (one example shown in Fig. 3b) has also been shown to affect radiative damping of their LSP resonances, playing thereby a crucial role in efficiency third-harmonic generation [52].

Fig. 3 shows the different metal nanostructures for improved the optical properties of nonlinear effects has used three- dimensional nanostructures, gold nanocups were choice for optical second harmonic generation improvement [53]. The nonlinear optical properties of an organic polymer has been related with a plasmonic gap to get adjust of SHG by voltage [54] (Fig. 3d). SHG of barium titanate-Au nanoparticles has been improved by a factor of more than 500 times compared with the bare of barium titanate [55] (Fig. 3e).

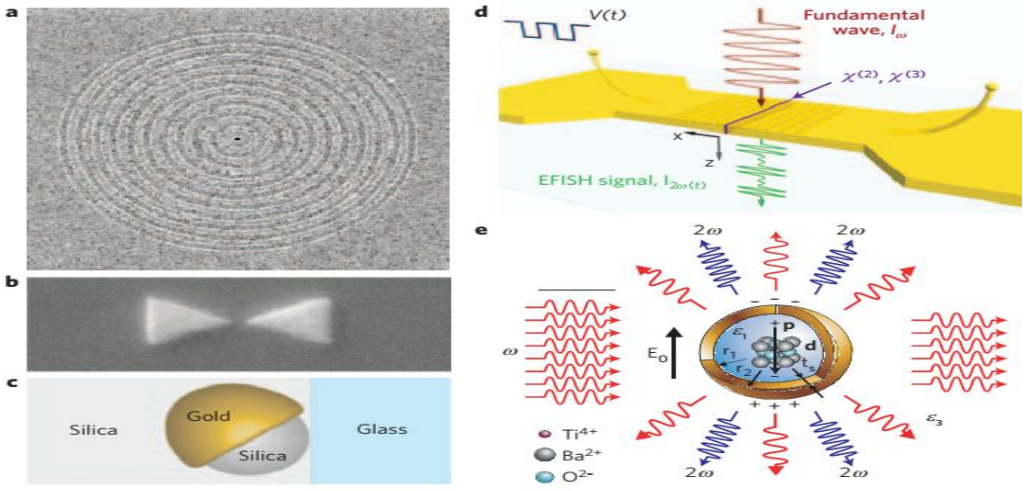

Fig. 3. Different metal nanostructures for improved the optical properties of nonlinear effects has used three- dimensional nanostructures. A. SHG improvement of nano-aperture in a silver film, enclosed by a circular grating. b, third-harmonic generation of gold bowtie antenna). c, SHG of gold nanocup. d, electric-field-induced SH generation by plasmonic grating and nanoslit filled with nonlinear polymer. e, SHG of barium titanate nanoparticle of radius r_1 and nonlinear coefficient tensor of d covered by gold shell of thickness ts and outer radius of r_2

4. SURFACE PLASMON IMPROVED NONLINEAR EFFECTS

Because of the centrosymmetry rule, the design of nanostructures with noncentrosymmetric shapes has become essential. Nowadays, both top-down and bottom-up approaches have been optimized for the fabrication of nanoparticles with excellent reproducibility. The SHG response from chemically synthesized and lithographed nanoparticles with various geometries has been investigated [56] (Fig. 4).

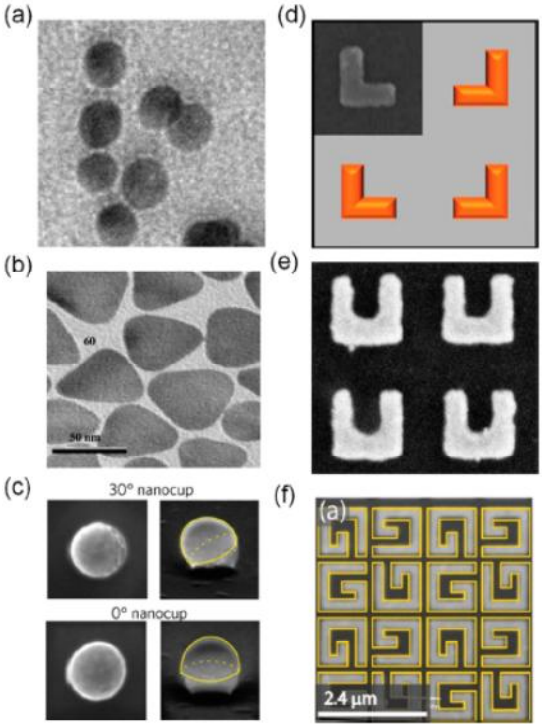

Fig. 4. Examples of structures in which the SHG has been studied. Chemically synthesized nanoparticles adapted from reference [124]: (a) 20 nm gold nanoparticles, (b) silver nanoprisms], and (c) gold nanocups]. Lithographed nanoparticles: (d) L-shaped nanoparticles, (e) gold split-rings, and (f) chiral G-shaped nanoparticles

Often any shape can be designed, and such geometries contain, for example, gold nanostars [57], silver triangular nanoprisms [58], holes in metallic films [59-63], curved nanorods [64], split-ring resonators with U-shape [65-67], metal_dielectric nanodisks [68], gold T-dimers [69], nanocups [70], chiral G-shaped nanoparticles [71-76], chiral helix [77-79], L-shaped nanoparticles [80-84], or gold nanotips [85-87]. These different nanoparticle shapes aggravate specific properties of the nonlinear response and were thus designed for different aims. For example, L-shaped nanoparticles are basic plasmonic elements with noncentrosymmetric shapes and are efficient to increase the typically SHG intensity in the backward and forward directions. Split-ring resonators support magnetic modes maintain also high SHG intensities, besides being the elementary constitutive elements for a huge several of metamaterials. Chiral nanostructures have also been designed; the SHG response from these structures based on the fairness of the incident light leading to the so-called SH circular dichroism [88,89]. Superchiral metasurfaces combine the chirality of light with that of nanostructures and induce strong SH intensities [90]. Besides the study of nanostructures, that of nanoholes in metal nanofilms has also been made as mutual systems in the sense of Babinet principle for nanostructures. The possibility to observe extraordinary light transmission, where the transmitted intensity is much higher than the one expected from the geometric aperture area, has driven this research [91]. In comparison with nanoparticles, nanoholes and nanocavities can support higher incident peak intensities due to the fast heat dissipation in the metallic film, resulting in a higher damage threshold. It is interesting to note that a noncentrosymmetric shape does not necessarily result in a stronger SHG intensity, and further symmetry issues can arise despite the lack of centrosymmetry. For example, the nonlinear efficiency of noncentrosymmetric decahedra with five fold symmetry is identical to that of centrosymmetric spheres with identical sizes due to the cancellation of the nonlinear emissions from their different facets [92]. A symmetry relation often encountered in this framework, and particularly in the case of nanoparticle arrays, is the mirror symmetry. If a mirror symmetry is actually present, then the SH wave propagating along the forward and backward directions is polarized in the symmetry plane due to the spatial reversal of the nonlinear polarization and cancels in the other direction [93]. A dramatic consequence arises when the nanoparticle array exhibits two orthogonal mirror planes: the SH intensity vanishes in these directions, although the constituting nanoparticles are not centrosymmetric [94]. This particularity must be kept in mind for the design of nanostructure arrays. It may also result in surprising observations for coupled nanostructures (Fig. 5).

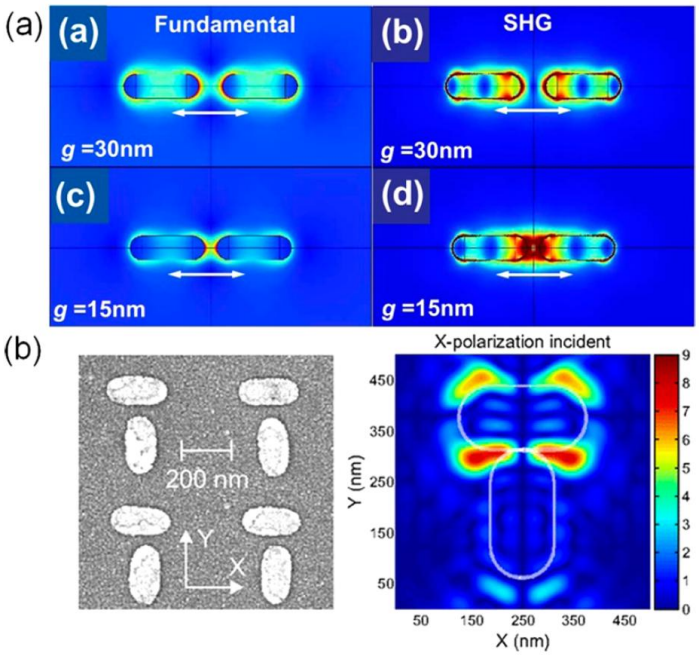

Fig. 5. SHG from coupled nanoparticles: (a) gold nanoantennas and (b) gold T-dimers. Panel (a) (adopted from ref. 69). Panel (b) (adopted from ref. 43)

One could naively think that the high fundamental field observed in narrow gaps [95] induces a strong SHG. Actually, this is not the case, and the reverse, the silencing of the SHG from plasmonic nanoantennas, has been pointed out [96]. Although the strong field enhancement observed in the gaps at the fundamental wavelength results indeed in a strong nonlinear polarization [97] the nonlinear polarization vectors standing at each sides of the nanogap are out of phase and their contributions to the SH wave tend to cancel out in the far-field region [98,99]. This silencing of the SHG response is partially suppressed in nanogaps with noncentrosymmetric geometries, as those observed in gold nanoparticle dimers with T-shapes [43] or structures composed of two arms with different sizes [100,101]. This silencing is a direct consequence of the symmetry properties of SHG and, as such, is not detected for third-order nonlinear optical processes such as THG and FWM. These examples further emphasize one more time the unique properties of SHG. Here, a clear separation has been made between the centrosymmetry breaking induced by the nanoparticle shapes and the electromagnetic fields. The distinction is, however, not unambiguously defined since both effects are deeply interconnected. The case of spherical nanoparticles is a good example to illustrate this remark. For the smallest nanoparticles, the origin of the SH response is their nonperfectly symmetric shape (Fig. 4a), but as the nanoparticle size increases, the role played by the retardation effects becomes more important [102]. The transition from a dipolar SH emission induced by shape effects to a quadrupolar SH emission induced by retardation is a good example of the interconnection between the geometry of the nanostructure (size, shape, etc.) and the properties of the electromagnetic fields at both the fundamental and SH frequencies [102].

5. POTENTIAL APPLICATIONS OF SHG IN NANOSTRUCTURES

5.1 Nonlinear Optical Characterization of Structural Properties

Indeed, as a consequence of the influence of centrosymmetry, SHG varies considerably with the nanostructure shape, opening the way to *in situ* ultrasensitive nonlinear optical characterization techniques. Indeed, SHG is able to reveal any small deviation from perfectly symmetric shapes [103,104] and small surface roughness [105]. This is very appealing since SHG can reveal defects that do not modify the linear response at all but are encoded in the SH emission pattern (see Fig. 6a) [105,106]. For some specific nanoparticle geometries, beam

shaping and polarization state definition are necessary for a good coupling between the incident laser field and LSPR, as demonstrated in the case of the nonlinear optical characterization of gold nanotips with cylindrical vector incident beams with azimuthal and radial polarizations (see Fig. 6b) [106].

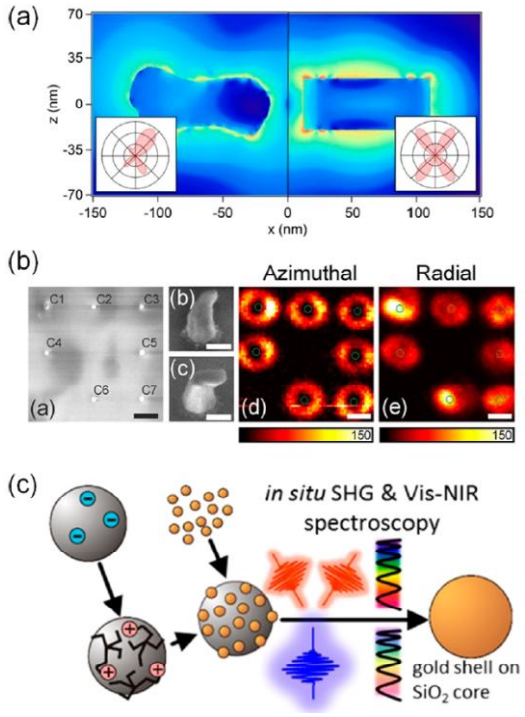

Fig. 6. Nonlinear optical characterization of plasmonic nanoparticles using SHG (a). Numerical study comparing the SHG from a realistic nanoantenna with that from an idealized one. (b) Imaging of gold nanotips using cylindrical vector incident beams. (c) In situ monitoring of gold nanoshell growth using SHG

What is even more interesting is that SHG can provide useful information on the chemical synthesis of plasmonic nanoparticles, beyond the characterization of finalized samples. Indeed, the in situ monitoring of the different synthesis steps is important for a good control of the final nanoparticle shapes and size dispersions [107,108]. For example, the growth of gold shells on silica cores has been simultaneously monitored with UV_visible spectroscopy and HRS during the chemical synthesis of gold nanoshells (see Fig. 6c) [107]. These experiments have shown that the SH intensity rises to a maximum before the complete closure of the gold shells. This was attributed to the surface roughness and the nonsymmetric hot spot distribution over the nanoparticle surface [108]. This approach has been also used for monitoring the chemical synthesis of gold nanostars [109] and gold nanoparticles aggregation [110] demonstrating its range of applications.

5.2 Laser Beam Characterization

The NLO is deeply connected with research in the physics of lasers. SHG from plasmonic nanostructures may therefore be used in laser beam characterization. We already mentioned that it is possible to tailor the incident laser beam properties in order to guarantee a strong coupling between the investigated nanostructures and the incident electromagnetic field, but the inverse is also true: it is possible to use SHG from single nanostructures to probe the properties of highly focused laser beams much below the diffraction limit with a high accuracy. Let us first consider the determination of the spatial features of the laser beam. Fig. 7a shows how the longitudinal component of a strongly converging Gaussian (HG00) beam can be probed with the SHG from single gold nanotips [111]. The tip is moved in the laser spot, and the map of the SH intensity reveals two positions for which the coupling between the gold nanotips and the incident laser beam is excellent. These positions correspond to the ones with a strong longitudinal component of the incident electric field, emphasizing that the vector nature of the incident electric field can be probed at the nanoscale using SHG [112]. On the other hand, the observation of SHG from plasmonic nanoparticles requires the use of ultrashort (femtosecond) laser systems. To satisfy the conjugated observable principle, ultrashort femtosecond pulses (~30 fs and shorter) have a very large bandwidth (up to several hundreds of nanometers). Due to the dispersive optical elements used in experimental setups, the different spectral components of femtosecond pulses do not reach the sample at the same time, and the SHG is not very efficient (see the green curves in Fig. 7b) [113,114]. Accanto et al. have proposed to use a preconditioning scheme, before the experimental setup, in order to compensate the unfavorable effects of dispersion in nonlinear plasmonic experiments [113,114]. After several optimization rounds, the SH intensity is increased by several orders of magnitude (see the black curves in Fig. 7b), demonstrating that the SHG from plasmonic nanoparticles can be used to check the temporal

features of femtosecond laser pulses with a spatial resolution of ~100 nm [113,114].

5.3 Nonlinear Plasmonic Sensing

Applications benefiting from the fundamentals and basic ideas exposed above can then be envisaged, like nonlinear plasmonic sensing. Before discussing how the SHG multipolar nature can be used in sensing, it is worth saying few words about the current developments in nonlinear plasmonic sensors. Indeed, one of the most promising applications in plasmonics is the sensing of chemical and biological entities, making use of the SPR-enhanced sensitivity [115-120]. Quickly, in the past, it has been realized that SHG from plasmonic nanostructures can be used to monitor chemical processes and to detect biological and chemical toxins with excellent sensitivity and selectivity [121]. SHG and HRS from gold nanoparticles were used to detect "spectroscopically silent" heavy metal ions (Pb2+) [122] diagnose single-base-mismatch DNA hybridization [121] selectively detect and identify Escherichia coli bacteria with gold nanorods, [123] detect Alzheimer's disease biomarkers [122] or detect breast cancer cells using the SHG from oval-shaped nanoparticles [124]. All these examples demonstrate the extensive versatility of the method for applications. They are based on the same simple scheme. The gold nanoparticles are first functionalized, that is, capped with specific molecules or biomolecules. The capping agent is selected for its high affinity with the targeted chemical/biological species in order to make chemical bonds between the nanoparticles. Since the SH signal from small nanoparticle aggregates strongly differs from the nonlinear signal from a collection of noninteracting nanoparticles, the presence of the target species induces a dramatic increase of the SH intensity.

Ray In his review on the second-order nonlinear optical properties of nanomaterials provides the reader with a very informative table, where he compares the detection limit of this approach with the detection limit of other assays based on nanostructures [125]. This comparative study reveals that SHG is very efficient for the detection of *Escherichia coli* bacteria or the tau protein but is less efficient than surface-enhanced Raman scattering [122] and real-time polymer chain reaction [126] for the detection of DNA/RNA. It is also less efficient than nanoparticle-based surface energy transfer [127] and electrochemical approaches for the detection of mercury [128]. These tests clearly show that SHG is a method of choice for plasmonic sensing and is appealing for the development of new strategies.

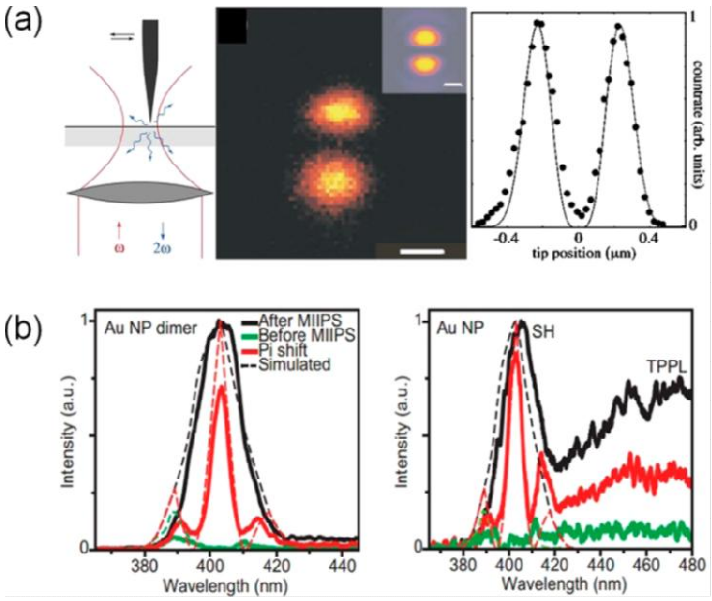

Fig. 7. Optical beam characterization: (a) longitudinal component of a strongly converging Gaussian (HG00) beam probed with the SHG from gold nanotips .(b) Optimization of the compression of femtosecond laser pulses using the SHG from single gold nanoparticles

6. THE DAMAGE THRESHOLD OF THE PLASMONIC NANOSTRUCTURES

The nonlinear systems means high power and strong laser pulses of the incident wavelength without the damage threshold of structures. The threshold condition define as the gain process of the laser intensities ($\sigma(I_\lambda)$) should be at least equal or greater than the lose process of the laser intensities ($\alpha(I_\lambda)$), according to the following equation

$$(\sigma(I_\lambda)) \geq (\alpha(I_\lambda)) \quad (3)$$

The threshold of the nanosystem depends on the some parameters such as the laser pulse duration (ł), the intensity of the laser (I_λ), pulse energy laser(E_0), the repetition rate of the pulse laser (T), and the composition of the nanostructures(X). The composition of the nanostructures(X) is one of the parameter that play important role in limiting the damage threshold. The repetition rate of the pulse laser (T) should be a significant because the low repetition rate of the pulse laser (T) is avoid the heating of plasmonic nanostructures system, as well as the spacing between the single pulses also avoid the heating of plasmonic nanostructures system [129,130].

7. CONCLUSIONS AND OUTLOOK

In conclusions, we have stressed the basics of SHG principle and the effect of symmetry in both the origin of the nonlinearity (local surface versus nonlocal bulk contributions) and the shape dependence of the scattered SH wave. We summed up the relationship between the specific properties of SHG from plasmonic nanostructures and some advanced applications. Regardless of considerable amount theoretical and experimental work devoted to the SHG from plasmonic nanostructures, the relative contributions of the conduction and core electrons has not yet been uniquely determined. This review has focused on nanostructures made of the most common plasmonic metals (gold, silver, copper, and aluminum).

This article review deals with second – harmonic generation of plasmonic nanostructures it consists of general introduction about the title in section 1, section 2 provides the basic informational (definition, mechanisms process and some equations) which related with nonlinear plasmonic. Section 3. Show the concept of second- harmonic generation (SHG) in nanostructures. Section 4. Review the nonlinear effects enhancement via surface plasmon and the potential applications of SHG in nanostructures was reported in section 5. Included three famous potential applications. The damage threshold of the nanostructures in section 6.

COMPETING INTERESTS

Author has declared that no competing interests exist.

REFERENCES

1. Plasmon hybridization model generalized to conductively bridged nanoparticle dimers, Lifei Liu, Yumin Wang, Zheyu Fang and Ke Zhao, J. Chem. Phys. 2013;139:064310.
   Available: http://dx.doi.org/10.1063/1.4817592
2. Linear and nonlinear optical properties of hybrid metallic–dielectric plasmonic nanoantennas, Mario Hentschel, Bernd Metzger, Bastian Knabe, Karsten Buse, and Harald Giessen, Beilstein J. Nanotechnol. 2016;7:111–120.
3. Nonlinear Optical Reflection from a Metallic Boundary, F. Brown, R. E. Parks, A. M. Sleeper, Phys. Rev. Lett. 1965;14:1029.
4. Franken PA, Hill AE, Peters CW, Weinreich G. Generation of optical harmonics. Phys. Rev. Lett. 1961;7:118.
5. Sipe JE, Stegeman GI. Surface polaritons: Electromagnetic waves at surfaces and interfaces, edited by V. M. Agranovich and D. L. Mills (North-Holland, Amsterdam; 1982.
6. Guidotti D, Driscoll TA, Gerritsen HJ. Second harmonic generation in centro-symmetric semiconductors. Solid State Commun. 1983;46:337.
7. Sipe JE, Moss DJ, van Driel HM. Phenomenological theory of optical second- and third-harmonic generation from cubic centrosymmetric crystals. Phys. Rev. B. 1987;35:1129.
8. Chen CK, de Castro ARB, Shen YR. Surface-enhanced second-harmonic generation. Phys. Rev. Lett. 1981;46:145.
9. Chen CK, Heinz TF, Ricard D, Shen YR. Surface-enhanced second-harmonic generation and Raman scattering. Phys. Rev. B. 1983;27.

10. Janz S, van Driel HM. Second-harmonic generation from metal surfaces. International J. Nonlinear Optical Phys. 1993;2.
11. Jha SS. Theory of optical harmonic generation at a metal surface. Phys. Rev. 1965;140:A2020.
12. Bloembergen N, Chang RK, Jha SS, Lee CH. Optical second-harmoni generation in reflection from media with inverse symmetry. Phys. Rev. 1968;174:813.
13. Rudnick J, Stern EA. Second-Harmoni radiation from metal surfaces. Phys. Rev. B. 1971;4:4272.
14. Eguiluz A, Quinn JJ. Hydrodynamic model for surface plasmons in metals and degenerate semiconductors. Phys. Rev. B. 1976;14:1347.
15. Sipe JE, So VCY, Fukui M, Stegeman GI. Analysis of second-harmonic generation at metal surfaces. Phys. Rev. B. 1980;21:4389.
16. Hua XM, Gersten JI. Theory of second-harmonic generation by small metal spheres. Phys. Rev. B. 1986;33:3756.
17. Maytorena JA, Luis Moch´an W, Mendoza BS. Hydrodynamic model for sum and difference frequency generation at metal surfaces. Phys. Rev. B. 1998;57:2580.
18. Guyot-Sionnest P, Chen W, Shen YR. General considerations on optical second-harmonic generation from surfaces and interfaces. Phys. Rev. B. 1986;33:8254.
19. Dadap JI, Shan J, Eisenthal KB, Heinz TF. Second-harmonic Rayleigh scattering from a sphere of centrosymmetric material. Phys. Rev. Lett. 1999;83:4045.
20. Stockman MI, Bergman DJ, Anceau C, Brasselet S, Zyss J. Enhanced second-harmonic generation by metal surfaces with nanoscale roughness: Nanoscale dephasing. Depolarization, and Correlations. Phys. Rev. Lett. 2004;92: 057402.
21. A classical theory for second-harmonic generation from metallic nanoparticles Yong Zeng, Walter Hoyer, Jinjie Liu, Stephan W. Koch, and Jerome V. Moloney Phys. Rev. B. 2009;79:235109.
22. Cooperative Enhancement of second-harmonic generation from a single CdS Nanobelt-Hybrid Plasmonic Structure, Xinfeng Liu, Qing Zhang, Wee Kiang Chong, Jing Ngei Yip, Xinglin Wen, Zhenpeng Li, Fengxia Wei, Guannan Yu, Qihua Xiong, and Tze Chien Sum, 2015 American Chemical Society, pp 5018–5026.
Available:http://dx.doi.org/10.1021/nn5072045
23. Second –harmonic imaging microscopy for visualizing biomolecular arrays in cells, tissues and organisms, Nat. Biotechnology, P.J. Campagnola and L.M. Loew. 2003;21:1356-1360.
Available:http://dx.doi.org/10.1038/nbt894
24. Generation of optical Harmonics, P.A. Franken, A.E. Hill, C.W. Peters, G. W. Reich, Phys. Rev. Lett. 1961;7:118-119.
Available:http://dx.doi.org/10.1103/physrevlett.7.118
25. Enhancing Second Harmonic Generation in Gold Nanoring Resonators Filled with Lithium Niobate, D. Lehr, J. Reinhold, I. Thiele, et al, Nano Letters. 2015;15:1025-1030.
Available:http://dx.doi.org/10.1021/nl5038819
26. High-efficiency second harmonic generation from a single hybrid ZnO nanowire/au plasmonic nano-oligomer, G. Grinblat, M. Rahmani, E. Cortes, et al Nano Letters. 2014;14:6660-6665.
Available:http://dx.doi.org/10.1021/nl503332f
27. Johnson JC, Yan H, Schaller RD, Petersen PB, Yang P, Saykally RJ. Near-field imaging of nonlinear optical mixing in single zinc oxide nanowires. Nano Lett. 2002;2:279–283.
28. Long JP, Simpkins BS, Rowenhorst DJ, Pehrsson PE. Far-field imaging of optical second-harmonic generation in single GaN nanowires. Nano Lett. 2007;7:831–836.
29. Dutto F, Raillon C, Schenk K, Radenovic A. Nonlinear optical response in single alkaline niobate nanowires. Nano Lett. 2011;11:2517–2521.
30. Sanatinia R, Anand S, Swillo M. Modal engineering of second-harmonic generation in single gap nanopillars. Nano Lett. 2014;14:5376–5381.
31. Boyd RW. Nonlinear optics 3rd edn (Academic, 2008).
32. Martti K, Anatoly VZ. Nonlinear plasmonics. Nature Photonic. 2012;6.
DOI: 10.1038/NPHOTON.2012.244
33. Zayats AV, Smolyaninov II, Maradudin AA. Nano-optics of surface plasmon polaritons. Phys. Rep. 2005;408:131–314.
34. Ren M, et al. Nanostructured plasmonic medium for terahertz bandwidth all-optical

switching. Adv. Mater. 2011;23:5540–5544.
35. Esteban R, Borisov AG, Nordlander P, Aizpurua J. Bridging quantum and classical plasmonics with a quantum-corrected model. Nature Commun. 2012;3:825.
36. García de Abajo FJ. Nonlocal effects in the plasmons of strongly interacting nanoparticles, dimers, and waveguides. J. Phys. Chem. C. 2008;112:17983–17987.
37. Novotny L, van Hulst N. Antennas for light. Nature Photon. 2011;5:83–90.
38. Argyropoulos C, Chen PY, D'Aguano G, Engheta N, Alu A. Boosting optical nonlinearities in epsilon-near-zero plasmonic channels. Phys. Rev. B. 2012;85:045129.
39. Wurtz GA, et al. Designed ultrafast optical nonlinearity in a plasmonic nanorod metamaterial enhanced by nonlocality. Nature Nanotech. 2011;6:107–111.
40. Dadap JI, Shan J, Eisenthal KB, Heinz TF. Second-harmonic Rayleigh scattering from a sphere of centrosymmetric material. Phys. Rev. Lett. 1999;83:4045–4048.
41. Dadap JI, Shan J, Heinz TF. Theory of optical second-harmonic generation from a sphere of centrosymmetric material: Small-particle limit. J. Opt. Soc. Am. B. 2004;21:1328–1347.
42. Vance FW, Lemon BI, Hupp JT. Enormous hyper-Rayleigh scattering from nanocrystalline gold particle suspensions. J. Phys. Chem. B. 1998;102:10091–10093.
43. Hao EC, Schatz GC, Johnson RC, Hupp JT. Hyper-Rayleigh scattering from silver nanoparticles. J. Chem. Phys. 2002;117:5963–5966.
44. Nappa J, Russier-Antoine I, Benichou E, Jonin C, Brevet PF. Second harmonic generation from small gold metallic particles: From the dipolar to the quadrupolar response. J. Chem. Phys. 2006;125:184712.
45. Butet J, et al. Interference between selected dipoles and octupoles in the optical second-harmonic generation from spherical gold nanoparticles. Phys. Rev. Lett. 2010;105:077401.
46. Butet J, et al. Optical second harmonic generation of single metallic nanoparticles embedded in a homogeneous medium. Nano Lett. 2010;10:1717–1721.
47. Optical second harmonic generation in plasmonic nanostructures: From Fundamental Principles to Advanced Applications, Jeremy Butet, Pierre-Francois Brevet, and Olivier J. F. Martin, American Chemical Society. 2015;9(11):10545–10562.
48. Bouhelier A, Beversluis M, Hartschuh A, Novotny L. Near-field second-harmonic generation induced by local field enhancement. Phys. Rev. Lett. 2003;90:013903.
49. Neacsu CC, Reider GA, Raschke MB. Second-harmonic generation from nanoscopic metal tips: Symmetry selection rules for single asymmetric nanostructures. Phys. Rev. B. 2005;71:201402.
50. Nahata A, Linke RA, Ishi T, Ohashi K. Enhanced nonlinear optical conversion from a periodically nanostructured metal film. Opt. Lett. 2003;28:423–425.
51. Danckwerts M, Novotny L. Optical frequency mixing at coupled gold nanoparticles. Phys. Rev. Lett. 2007;98:026104.
52. Marinica DC, Kazansky AK, Nordlander P, Aizpurua J, Borisov AG. Quantum plasmonics: Nonlinear effects in the field enhancement of a plasmonic nanoparticle dimer. Nano Lett. 2012;12:1333–1339.
53. Hanke T, et al. Tailoring spatiotemporal light confinement in single plasmonic nanoantennas. Nano Lett. 2012;12:992–996.
54. Zhang Y, Grady NK, Ayala-Orozco C, Halas NJ. Three-dimensional nanostructures as highly efficient generators of second harmonic light. Nano Lett. 2011;11:5519–5523.
55. Cai W, Vasudev AP, Brongersma ML. Electrically controlled nonlinear generation of light with plasmonics. Science. 2011;333:1720–1723.
56. Pu Y, Grange R, Hsieh C-L, Psaltis D. Nonlinear optical properties of core-shell nanocavities for enhanced second-harmonic generation. Phys. Rev. Lett. 2010;104:207402.
57. Park I-Y, et al. Plasmonic generation of ultrashort extreme-ultraviolet light pulses. Nature Photon. 2011;5:677–681.
58. Singh AK, Senapati D, Neely A, Kolawole G, Hawker C, Ray CP. Nonlinear optical properties of triangular silver nanomaterials. Chem. Phys. Lett. 2009;481:94–98.
59. Schön P, Bonod N, Devaux E. Wenger J. Rigneault H, Ebbesen TW, Brasselet S. Enhanced second-harmonic generation from individual metallic nanoapertures. Opt. Lett. 2010;35:4063–4065.

60. Xu T, Jiao X, Zhang GP, Blair S. Second-harmonic emission from sub-wavelength apertures: Effects of aperture symmetry and lattice arrangement. Opt. Express. 2007;15:13894–13906.
61. Salomon A, Zielinski M, Kolkowski R, Zyss J, Prior Y. Size and shape resonances in second harmonic generation from silver nanocavities. J. Phys. Chem. C. 2013;117: 22377–22382.
62. Kolkowski R, Szeszko J, Dwir B, Kapon E, Zyss J. Effects of surface Plasmon Polariton-mediated interactions on second harmonic generation from assemblies of pyramidal metallic nano-cavities. Opt. Express. 2014;22:30592–30606.
63. Kim MK, Sim H, Yoon SJ, Gong SH, Ahn CW, Cho YH, Lee YH. Squeezing photons into a point-like space. Nano Lett. 2015;15: 4102–4107.
64. Belardini A, Larciprete MC, Centini M, Fazio E, Sibilia C. Circular Dichroism in the optical second-harmonic emission of curved gold metal nanowires. Phys. Rev. Lett. 2011;107:257401.
65. Klein MW, Enkrich C, Wegener M, Linden, S. Second- harmonic generation from magnetic metamaterials. Science. 2006;313:502–504.
66. Ciracì C, Poutrina E, Scalora M, Smith DR. Origin of second-harmonic generation enhancement in optical split-ring resonators. Phys. Rev. B: Condens. Matter Mater. Phys. 2012;85:201403(R).
67. Linden S, Niesler FBP, Förstner J, Grynko Y, Meier T, Wegener M. Collective effects in second-harmonic generation from split-ring-resonator arrays. Phys. Rev. Lett. 2012;109:015502.
68. Kruk S, Weismann M, Bykov AY, Mamonov EA, Kolmychek IA, Murzina T, Panoiu NC, Neshev DN, Kivshar YS. Enhanced magnetic second-harmonic generation from resonant metasurfaces. ACS Photonics. 2015;2:1007–1012.
69. Canfield BK, Husu H, Laukkanen J, Bai BF, Kuittinen M, Turunen J, Kauranen M. Local field asymmetry drives second-harmonic generation in noncentro-symmetric nanodimers. Nano Lett. 2007;7:1251–1255.
70. Zhang Y, Grady NK, Ayala-Orozco C, Halas NJ. Three- dimensional nanostructures as highly efficient generators of second harmonic light. Nano Lett. 2011;11:5519–5523.
71. Valev VK, Smisdom N, Silhanek AV, De Clercq B, Gillijns W, Ameloot M, Moshchalkov VV, Verbiest T. Plasmonic ratchet wheels: Switching circular dichroism by arranging chiral nanostructures. Nano Lett. 2009;9:3945–3948.
72. Valev VK, Volodin A, Silhanek AV, Gillijns W, De Clercq B, Jeyaram Y, Paddubrouskaya H, Biris CG, Panoiu NC, Aktsipetrov OA, et al. Plasmons reveal the direction of magnetization in NickelN. ACS Nano. 2011;5:91–96.
73. Valev VK. Characterization of nanostructured plasmonic surfaces with second harmonic generation. Langmuir. 2012;28:15454–15471.
74. Mamonov EA, Kolmychek IA, Vandendriessche S, Hojeij M, Ekinci Y, Valev VK, Verbiest T, Murzina TV. Anisotropy versus circular dichroism in second harmonic generation from fourfold symmetric arrays of g-shaped nanostructures. Phys. Rev. B: Condens. Matter Mater. Phys. 2014;89:121113(R).
75. Valev VK, Baumberg JJ, Sibilia C, Verbiest T. Chirality and chiroptical effects in plasmonic nanostructures: Fundamentals, recent progress, and outlook. Adv. Mater. 2013;25:2517–2534.
76. Valev VK, Silhanek AV, Verellen N, Gillijns W, Van Dorpe P, Aktsipetrov OA, Vandenbosch GAE, Moshchalkov VV, Verbiest T. Asymmetric optical second-harmonic generation from chiral G-shaped gold nanostructures. Phys. Rev. Lett. 2010;104:127401.
77. Valev VK, De Clercq B, Zheng X, Denkova D, Osley EJ, Vandendriessche S, Silhanek AV, Volskiy V, Warburton PA, Vandenbosch GAE, et al. The role of Chiral local field enhancements below the resolution limit of second harmonic generation microscopy. Opt. Express. 2012;20:256–264.
78. Decker M, Ruther M, Kriegler CE, Zhou J, Soukoulis CM, Linden S, Wegener M. Strong optical activity from twisted-cross photonic metamaterials. Opt. Lett. 2009;34:2501.
79. Huttunen MJ, Bautista G, Decker M, Linden S, Wegener M, Kauranen M. Nonlinear Chiral imaging of subwavelength-sized twisted-cross gold nanodimers [Invited]. Opt. Mater. Express. 2011;1:46–56.

80. Kujala S, Canfield BK, Kauranen M, Svirko Y, Turunen J. Multipole interference in the second-harmonic optical radiation from gold nanoparticles. Phys. Rev. Lett. 2007;98:167403.
81. Canfield BK, Kujala S, Jefimovs K, Svirko Y, Turunen J, Kauranen M. A macroscopic formalism to describe the second-order nonlinear optical response of nanostructures. J. Opt. A: Pure Appl. Opt. 2006;8:S278–S284.
82. Czaplicki R, Zdanowicz M, Koskinen K, Laukkanen J, Kuittinen M, Kauranen M. Dipole limit in second- harmonic generation from arrays of gold nanoparticles. Opt. Express. 2011;19: 26866–26871.
83. Kujala S, Canfield BK, Kauranen M, Svirko Y, Turunen J. Multipolar analysis of second-harmonic radiation from gold nanoparticles. Opt. Express. 2008;16: 17196–17208.
84. Neacsu CC, Reider GA, Raschke MB. Second- harmonic generation from nanoscopic metal tips: Symmetry selection rules for single asymmetric nanostructures. Phys. Rev. B: Condens. Matter Mater. Phys. 2005;71:201402(R).
85. Anderson A, Deryckx KS, Xu XG, Steinmeyer G, Raschke MB. Few-femtosecond plasmon dephasing of a single metallic nanostructure from optical response function reconstruction by interferometric frequency resolved optical gating. Nano Lett. 2010;10:2519–2524.
86. Reichenbach P, Horneber A, Gollmer DA, Hille A, Mihaljevic J, Schäfer C, Kern DP, Meixner AJ, Zhang D, Fleischer M, et al. Nonlinear optical point light sources through field enhancement at metallic nanocones. Opt. Express. 2014;22:15484–15501.
87. Bertolotti M, Belardini A, Benedetti A, Sibilia C. Second harmonic circular dichroism by self-assembled metasurfaces [Invited]. J. Opt. Soc. Am. B. 2015;32: 1287–1293.
88. Kolkowski R, Petti L, Rippa M, Lafargue C, Zyss J. Octupolar plasmonic meta-molecules for nonlinear chiral watermarking at subwavelength scale. ACS Photonics. 2015;2:899–906.
89. Valev VK, Baumberg JJ, de Clercq B, Braz N, Zheng X, Osley EJ, Vandendriessche S, Hojeij M, Blejean C, Mertens J, et al. Nonlinear superchiral meta-surfaces: Tuning chirality and disentangling non-reciprocity at the nanoscale. Adv. Mater. 2014;26:4074–4081.
90. van Nieuwstadt JAH, Sandtke M, Harmsen RH, Segerink FB, Prangsma JC, Enoch S, Kuipers L. Strong modification of the nonlinear optical response of metallic subwavelength hole arrays. Phys. Rev. Lett. 2006;97:146102.
91. Russier-Antoine I, Duboisset J, Bachelier G, Benichou E, Jonin C, Del Fatti N, Vallée F, Sánchez-Iglesias A, Pastoriza-Santos I, Liz-Marzan LM, et al. Symmetry cancellations in the quadratic hyperpolarizability of non-centrosymmetric gold decahedra. J. Phys. Chem. Lett. 2010;1:874.
92. Benedetti A, Centini M, Bertolotti M, Sibilia C. Second harmonic generation from 3d nanoantennas: On the surface and bulk contributions by far-field pattern analysis. Opt. Express. 2011;19:26752–26727.
93. Husu H, Siikanen R, Mäkitalo J, Lehtolahti J, Laukkanen J, Kuittinen M, Kauranen M. Metamaterials with tailored nonlinear optical response. Nano Lett. 2012;12:673–677.
94. Kottmann JP, Martin OJF. Plasmon resonant coupling in metallic nanowires. Opt. Express. 2001;8:655–663.
95. Berthelot J, Bachelier G, Song M, Rai P, Colas des Francs G, Dereux A, Bouhelier A. Silencing and enhancement of second-harmonic generation in optical gap antennas. Opt. Express. 2012;20:10498–10508.
96. Slablab A, Le Xuan L, Zielinski M, de Wilde Y, Jacques V, Chauvat D, Roch JF. Second-harmonic generation from coupled plasmon modes in a single dimer of gold nanospheres. Opt. Express. 2012;20:220–227.
97. de Ceglia D, Vincenti MA, de Angelis C, Locatelli A, Haus JW, Scalora M. Role of antenna modes and field enhancement in second harmonic generation from dipole nanoantenna. Opt. Express. 2015;23: 1715–1729.
98. Biswas S, Liu X, Jarrett JW, Brown D, Pustovit V, Urbas A, Knappenberger KL, Jr.; Nealey PF, Vaia RA. Nonlinear chiro-optical amplification by plasmonic nanolens arrays formed via directed assembly of gold nanoparticles. Nano Lett. 2015;15:1836–1842.
99. Nappa J, Revillod G, Russier-Antoine I, Benichou E, Jonin C, Brevet PF. Electric dipole origin of the second harmonic

generation of Sm all metallic particles. Phys. Rev. B: Condens. Matter Mater. Phys. 2005;71:165407.
100. Bachelier G, Russier-Antoine I, Benichou E, Jonin C, Brevet PF. Multipolar second-harmonic generation in noble metal nanoparticles. J. Opt. Soc. Am. B. 2008;25:955–960.
101. Butet J, Thyagarajan K, Martin OJF. Ultrasensitive optical shape characterization of gold nanoantennas using second harmonic generation. Nano Lett. 2013;13: 1787–1792.
102. Bautista G, Huttunen MJ, Mäkitalo J, Kontio JM, Simonen J, Kauranen M. Second-harmonic generation imaging of metal nano-objects with cylindrical vector beams. Nano Lett. 2012;12:3207–3212.
103. Liz-Marzán LM. Tailoring surface plasmons through the morphology and assembly of metal nanoparticles. Langmuir. 2006;22: 32–41.
104. Eustis S, El-Sayed MA. Why gold nanoparticles are more precious than pretty gold: Noble metal surface plasmon resonance and its enhancement of the radiative and nonradiative properties of nanocrystals of different shapes. Chem. Soc. Rev. 2006;35:209–217.
105. Sauerbeck C, Haderlein M, Schürer B, Braunschweig B, Peukert W, Taylor RN. K. Shedding light on the growth of gold nanoshells. ACS Nano. 2014;8:3088–3096.
106. Senapati D, Singh AK, Khan SA, Senapati T, Ray CP. Probing real time gold nanostar formation process using two-photon scattering spectroscopy. Chem. Phys. Lett. 2011;504:46–51.
107. Russier-Antoine I, Huang J, Benichou E, Bachelier G, Jonin C, Brevet PF. Hyper Rayleigh scattering of protein-mediated gold nanoparticles aggregates. Chem. Phys. Lett. 2008;450:345.
108. Bouhelier A, Beversluis M, Hartschuh A, Novotny L. Near-field second-harmonic generation induced by local field enhancement. Phys. Rev. Lett. 2003;90: 013903.
109. Accanto N, Nieder JB, Piatkowski L, Castro-Lopez M, Pastorelli F, Brinks D, van Hulst NF. Phase control of femtosecond pulses on the nanoscale using second harmonic nanoparticles. Light: Sci. Appl. 2014;3:e143.
110. Accanto N, Piatkowski L, Renger J, van Hulst NF. Capturing the optical phase response of nanoantennas by coherent second-harmonic microscopy. Nano Lett. 2014;14:4078–4082.
111. Lakowicz JR. Radiative decay engineering: Biophysical and biomedical applications. Anal. Biochem. 2001;298:1–24.
112. Anker JN, Hall WP, Lyandres O, Shah NC, Zhao J, Van Duyne RP. Biosensing with plasmonic nanosensors. Nat. Mater. 2008;7:442–452.
113. Mayer KM, Hafner JH. Localized surface plasmon resonance sensors. Chem. Rev. 2011;111:3828–3857.
114. Liu N, Tang ML, Hentschel M, Giessen H, Alivisatos AP. Nanoantenna-enhanced gas sensing in a single tailored nanofocus. Nat. Mater. 2011;10:631.
115. Mock JJ, Smith DR, Schultz S. Local refractive index dependence of plasmon resonance spectra from individual nanoparticles. Nano Lett. 2003;3:485–491.
116. McFarland AD, van Duyne RP. Single silver nanoparticles as real-time optical sensors with zeptomole sensitivity. Nano Lett. 2003;3:1057–1062.
117. Raschke G, Kowarik S, Franzl T, Soennichsen C, Klar TA, Feldmann J. Biomolecular recognition based on single gold nanoparticle light scattering. Nano Lett. 2003;3:935–938.
118. Acimovic SS, Kreuzer MP, Gonzalez MU, Quidant R. Plasmon near-field coupling in metal dimers as a step toward single-molecule sensing. ACS Nano. 2009;3: 1231–1237.
119. Ray PC. Size and shape dependent second order nonlinear optical properties of nanomaterials and their application in biological and chemical sensing. Chem. Rev. 2010;110:5332–5365.
120. Kim Y, Johnson RC, Hupp JT. Gold nanoparticle-based sensing of "Spectroscopically Silent" heavy metal ions. Nano Lett. 2001;1:165–167.
121. Ray PC. Diagnostics of single base-mismatch DNA hybridization on gold nanoparticles by using the Hyper-Rayleigh scattering technique. Angew. Chem. Int. Ed. 2006;45:1151–1154.
122. Singh AK, Senapati D, Wang S, Griffin J, Neely A, Candice P, Naylor KM, Varisli B, Kalluri JR, Ray PC. Gold nanorod based selective identification of *Escherichia coli* bacteria using two-photon Rayleigh scattering spectroscopy. ACS Nano. 2009;3:1906–1912.

123. Neely A, Perry C, Varisli B, Singh A, Arbneshi T, Senapati D, Kalluri JR, Ray PC. Ultrasensitive and highly selective detection of Alzheimer's disease biomarker using two-photon Rayleigh scattering properties of gold nanoparticle. ACS Nano. 2009;3:2834–2840.
124. Lu W, Arumugam SR, Senapati D, Singh AK, Arbneshi T, Khan SA, Yu H, Ray PC. Multifunctional oval shape gold nanoparticle based selective detection of breast cancer cells using simple colorimetric and highly sensitive two-photon scattering. ACS Nano. 2010;4: 1739–1749.
125. Cao YWC, Jin RC, Mirkin CA. Nanoparticles with Raman spectroscopic fingerprints for DNA and RNA detection. Science. 2002;297:1536.
126. Abe A, Inoue K, Tanaka T, Kato J, Kajiyama N, Kawaguchi R, Tanaka S, Yoshiba M, Kohara M. Quantitation of hepatitis B virus genomic DNA by real-time detection PCR. J. Clin. Microbiol. 1999;37: 2899.
127. Darbha GK, Ray A, Ray PC. Gold nanoparticle-based miniaturized nano-material surface energy transfer probe for rapid and ultrasensitive detection of mercury in soil, water, and fish. ACS Nano. 2007;1:208.
128. Jena BK, Raj CR. Gold nanoelectrode ensembles for the simultaneous electrochemical detection of ultratrace arsenic, mercury, and copper. Anal. Chem. 2008;80:4836.
129. Summers SM, Ramm AS, Kling MK, Flanders BN, Herrero CA. Optical damage threshold of Au nanowires in strong femtosecond laser fields. Optics Express; 2014.
130. Ozturk B, Flanders BN, Grischkowsky DR, Mishima TD. Single-step growth and low resistance interconnecting of gold nanowires. Nanotechnology. 2007;18: 175707.

Peer-review history:
The peer review history for this paper can be accessed here:
http://sciencedomain.org/review-history/15966